ChemComm

COMMUNICATION

View Article Online
View Journal | View Issue



Cite this: *Chem. Commun.*, 2022, **58**, 12200

Received 13th January 2022,
Accepted 10th October 2022

DOI: 10.1039/d2cc00239f

rsc.li/chemcomm



# Sequence-complementarity dependent co-assembly of phosphodiester-linked aromatic donor–acceptor trimers†

Nadeema Appukutti, [a] Alex H. de Vries, [b] Prashant G. Gudeangadi, [a] Bini R. Claringbold,[a] Michelle D. Garrett,[c] Michael R. Reithofer [d] and Christopher J. Serpell *[a]

**We have created sequenced phosphoester-linked trimers of aromatic donor/acceptors which participate in charge-transfer interactions. Each sequence displays characteristic self-assembly, and complementary sequences interact with each other to produce new nanostructures and thermochromism. This paves the way towards new functional nanomaterials which make bio-analogous use of sequence to tune structure.**

Sequence is the defining factor in the folding and self-assembly of biomolecules to create the functional superstructures which underpin biochemistry. On this basis, the integration of sequence into supramolecular and polymer chemistry has the potential to open up new possibilities for recapitulation of pseudobiological function in synthetic chemistry.[1]

Aromatic donor–acceptor (DA) interactions,[2] involving electron—rich donors, such as dialkoxynaphthalene (**DAN**) and electron—poor acceptors, such as naphthalene diimide (**NDI**) have been used widely in synthetic supramolecular chemistry,[3–7] but are rare in biology in which hydrophobic collapse and hydrogen bonding dominate. Aromatic DA interactions have been used to create chains which are capable of directed folding and self-assembly. For example, amide-linked trimers of **DAN** and **NDI** fold according to sequence,[8] while longer alternating systems fold and interact,[9] and DA interactions have also been used to read oligomer sequences.[10] Homooligomeric DA chains can be interweaved to create discrete complexes[11–13] but efforts on integrating sequence in oligomers have focused on hydrogen bonding,[14] metal coordination,[15] and reversible covalent interactions.[16] Integration of sequence into extended self-assembly of DA oligomers therefore raises the possibility of creating biopolymer-like superstructures using chemical motifs rare in biology. Such self-assembled aromatic materials could find applications in nanoelectronics[17] and light harvesting.[18]

The phosphodiester backbone of nucleic acids provides an attractive platform for the creation of sequence-defined molecules because of the outstanding efficiency of the automated phosphoramidite synthesis which permits creation of polymers of >100 monomer units long.[19,20] DA interactions have been integrated into DNA itself,[21] and the phosphodiester backbone has been used in development of various π-stacked folded and self-assembled systems, generating significant complexity from oligomers as short as trimers.[22,23] Since aromatic donor and

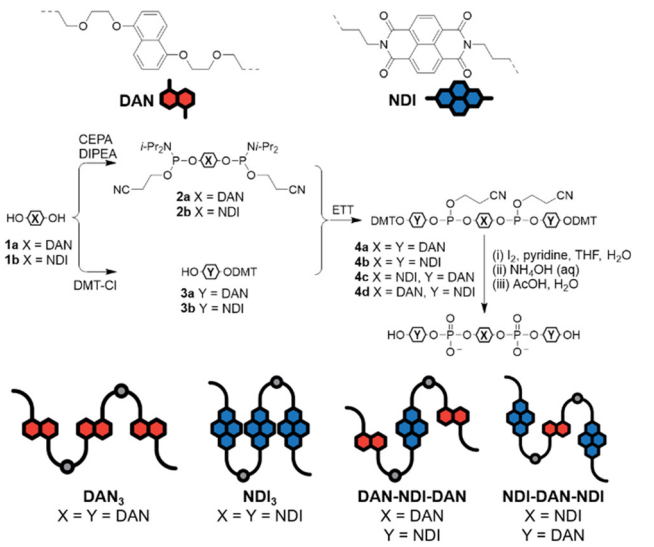


Scheme 1 Synthesis of phosphodiester trimers **DAN$_3$**, **NDI$_3$**, **DAN-NDI-DAN**, and **NDI-DAN-NDI**.

[a] *School of Chemistry and Forensic Science, Ingram Building, University of Kent, Canterbury, Kent, CT2 7NH, UK. E-mail: C.J.Serpell@kent.ac.uk*
[b] *Groningen Biomolecular Sciences and Biotechnology Institute and Zernike Institute for Advanced Materials, University of Groningen, Nijenborgh 7, 9747 AG Groningen, The Netherlands*
[c] *School of Biosciences, Stacey Building, University of Kent, Canterbury, Kent, CT2 7NJ, UK*
[d] *Dept. of Inorganic Chemistry, University of Vienna, Wahringer Strabe. 42, 1090 Vienna, Austria*

† Electronic supplementary information (ESI) available: Synthetic protocols and further analytical data. See DOI: https://doi.org/10.1039/d2cc00239f

acceptor units are complementary in a supramolecular sense, they reflect the hydrogen-bonded complementarity of nucleobases, and their sequence in a chain could therefore be used to control self-assembly. We now report that the extended self-assembly of phosphodiester-linked trimers of **DAN** and **NDI** is sequence-determined, and can be modified through complementarity of sequences. This provides an opportunity to develop polymers in which information-rich sequences control their resultant nanostructures, creating synthetic, bio-orthogonal analogues to DNA hybridisation, which could be used in nanoelectronics or light harvesting.

**DAN** and **NDI**-containing phosphodiester-linked trimers were constructed in a symmetrical building-outwards strategy, in four sequences – **$DAN_3$**, **$NDI_3$**, **DAN-NDI-DAN**, and **NDI-DAN-NDI** (Scheme 1). Monomers were constructed by attaching short spacers at either end of the aromatic units, terminated in hydroxyl units which could be used later to form phosphodiester linkages. The **DAN** diol monomer **1a** was synthesised by reacting 1,5-dihydroxynaphthalene with chloroethyl ethanol (52% yield) and the **NDI** diol **1b** was synthesised reacting 1,4,5,8-naphthalene-tetracarboxylic dianhydride and 3-aminopropanol in water, expediting a reported synthesis[24] by heating in a microwave giving the product in 70% yield and high purity. The central monomers were converted into doubly activated phosphoramidites **2a** and **2b** using cyanoethyl diisopropylchlorophosphoramidite (CEPA) in basic conditions, while different portions of **1a** and **1b** were dimethoxytrityl (DMT)-protected on just one hydroxyl to give the terminal monomers **3a** and **3b**. **2a** and **2b** were then activated immediately after synthesis with ethylthiotetrazole (ETT) and reacted separately with each of **3a** and **3b** to obtain DMT and cyanoethyl-protect phosphite triester-linked trimers in the desired sequences (**4a–d**). These were converted into phosphodiesters by iodine oxidation, giving a stable, organic soluble compounds which were purified by column chromatography. The cyanoethyl groups were removed under basic conditions, and final removal of the terminal DMT groups was achieved in 80% acetic acid, yielding **$DAN_3$**, **$NDI_3$**, **DAN-NDI-DAN**, and **NDI-DAN-NDI** in 37–53% isolated yields. NMR analysis (Fig. S1–S4, ESI†) was consistent with expected materials, but complicated by self-assembly. We were able to confirm identity by mass spectrometry (Fig. S5–S8, ESI†). Molecular dynamics (MD) simulations using a modification of the united-atom Gromos force field,[25] which is well parameterised for aromatic DA interactions,[26] indicated that the preferred conformations of all three trimers as isolated molecules were folded, with the mixed trimers displaying an overall S-shape which permitted expected DA interactions between the **DAN** donors and **NDI** acceptors (Fig. 1 and Fig. S27, ESI†). Whether these conformations would be seen experimentally would depend upon competing self-assembly.

UV-visible spectroscopy is a valuable tool in characterisation of the supramolecular chemistry of **DAN/NDI** complexes because the DA interaction can give rise to a charge transfer (CT) band with a peak at around 525 nm, giving the solutions a red–purple colour. The absorption spectra of the homotrimers **$DAN_3$** and **$NDI_3$** were recorded in water, and in tris-borate-EDTA (TBE), and tris-acetate-magnesium (TAMg) buffers (Fig. 2a, b and Fig. S9, S10, ESI†). The magnesium-containing buffer was

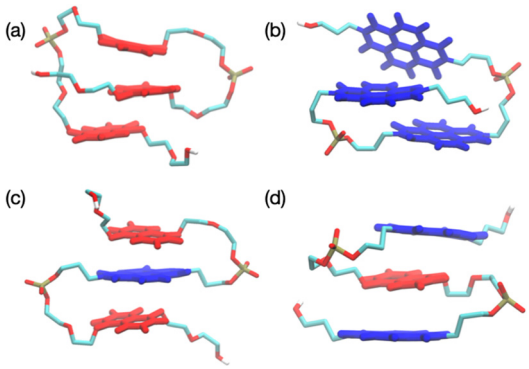


Fig. 1 MD snapshots of dominant conformations of (a) **$DAN_3$** (representing 26% of structures), (b) **$NDI_3$** (20%), (c) **DAN-NDI-DAN** (73%), and (d) **NDI-DAN-NDI** (76%) in water as individual molecules. **DAN** and NDI cores are highlighted by colouring them red and blue, respectively. Water and counter ions are not shown.

employed since the presence of the divalent cation can have dramatic effects upon the self-assembly of oligophosphates.[20,27] The yellow solutions gave absorption spectra characteristic of their respective aromatic units (250–350 nm for **DAN**, 370–400 nm for **NDI**), with the buffer systems making minimal difference. Both **DAN-NDI-DAN** and **NDI-DAN-NDI** gave purple solutions at 250 μM in water, TBE, or TAMg (Fig. 2c, d and Fig. S12, S13, ESI†), as would expected since they contain both donor and acceptor aromatics and could fold or self-assemble to satisfy DA interactions. The UV-visible spectra of both of the heterotrimers exhibited the CT band absorbances (450–700 nm) and no significant changes were observed for the different buffers or temperatures. The stable CT absorbance at 45 °C suggests that DA complex formation in these compounds is stable, while the consistency between buffers shows that the aromatic DA interactions and hydrophobic effect outweigh aspects of phosphate–phosphate repulsion. The CT band intensity was greater in **DAN-NDI-DAN** than in **NDI-DAN-NDI**; this absorption difference might be a result of **NDI** being a potent π-conjugated electron acceptor, while **DAN** is a relatively mediocre donor (2 : 1 **DAN** : **NDI** complexes being more

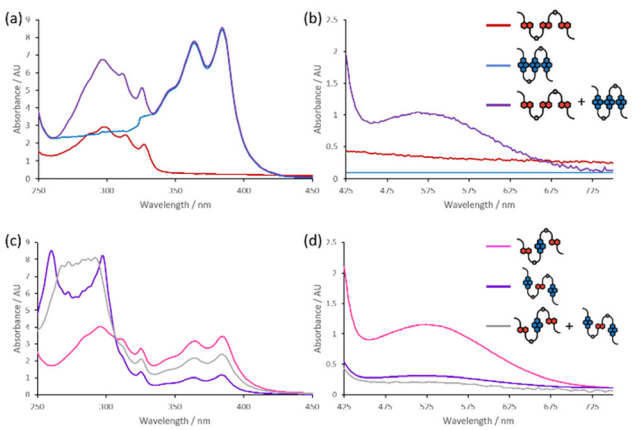


Fig. 2 UV-visible absorbance spectra (water, 20 °C, 250 μM) of (a and b) homotrimers and heterotrimers (c and d) highlighting typical **DAN/NDI** absorption bands (a and c) and charge transfer bands (b and d).

favoured than the inverse[28]) When more **DAN** units are present in the chain, the donor ability increases to fulfil the acceptance capacity of **NDI**, but when there are more **NDI** units present, they each operate at a lower relative capacity.

The self-assembly of the trimers was examined by atomic force microscopy (AFM) and transmission electron microscopy (TEM), as deposited from water (Fig. 3). In all cases, extended self-assembly was seen, and the findings were therefore compared with atomistic MD simulations of 48 trimer molecules in explicit water (Fig. 3 and Fig. S28, S29, ESI†). Deposition of **$DAN_3$** resulted in a film, with spherical protrusions of 6–20 nm in height (average 10.1 nm) and 100–150 nm in diameter. Modelling described an uneven flat layer 2–3 nm wide with the phosphate groups exposed. This is consistent with formation of the film as a bilayer, with the round protrusions being fully or partially formed vesicles developing from or collapsing into the bilayer. AFM and TEM of **$NDI_3$** showed a dense network of angular, elongated structures, averaging 7.1 nm in height and of various lengths between 150 and 600 nm. In contrast to the smooth perimeter of the **$DAN_3$** MD model aggregate, **$NDI_3$** formed finer, more angular structures, in line with the experimental data. AFM and TEM of **DAN-NDI-DAN** revealed small assemblies, with jagged edges, of average height 1.8 nm and diameter 88 nm – the small height is consistent with the interphosphate distance seen in the MD model of the same molecules which produced small branched sheets. AFM imaging of **NDI-DAN-NDI** showed smooth-edged particles and flakes (7.9 nm average height) of various diameters, including areas of continuous film at the same constant height, with some evidence of texture. TEM revealed this texture in more detail – the film has a sponge-like texture with distances of *ca.* 15 nm separating the higher contrast regions. MD simulations gave highly branched aggregates, which could fit with the network forming the solid part of the sponge-like aggregate.

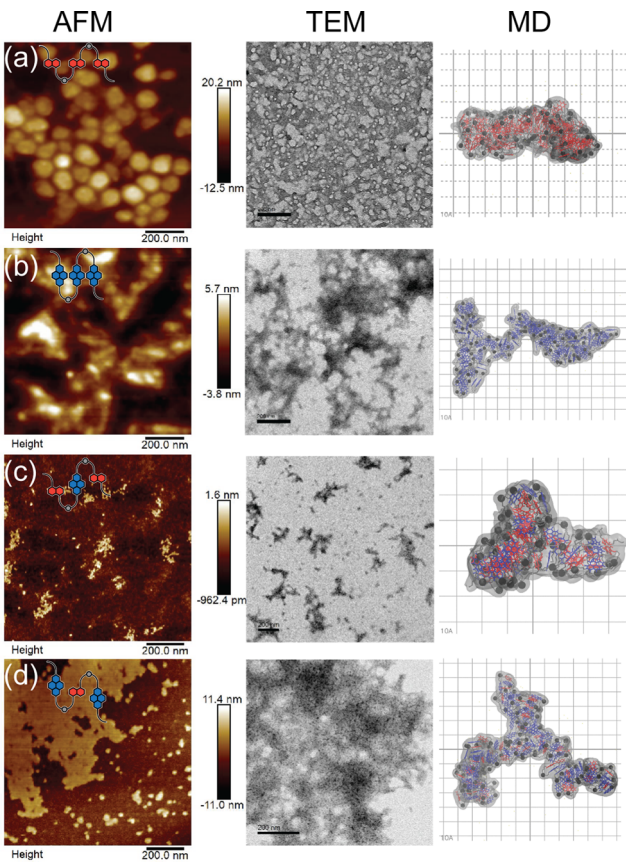


Fig. 3 AFM, TEM, and MD modelling of (a) **$DAN_3$** (b) **$NDI_3$** (c) **DAN-NDI-DAN** (d) **NDI-DAN-NDI**. Red units in the MD = **DAN**; blue = NDI; dark spheres = phosphates. van der Waals surface shown as a transparent envelope. Further AFM and TEM: Fig S15–S18 and S21–S24 (ESI†).

In all these cases, although the MD models exhibited some characteristic distances, overall morphologies, and short-range structural motifs, there was very little long range order, in contrast to what has been recently reported in a similar system.[9] Our results are in line with historical observations of conformational variation in donor–acceptor aromatic foldamers,[28] and make intuitive sense given the high degree of freedom imparted by the unconstrained 3–5 atom spacers between the aromatic units and the phosphates.

When the homotrimers **$DAN_3$** and **$NDI_3$** were mixed together in a 1 : 1 ratio in water, the solution turned from yellow to deep purple, and the CT band was seen in the UV-visible spectrum, indicating that the two systems were associating through complementary, spatially localised, donor–acceptor interactions. This CT band remained constant from room temperature up to 45 °C, evidencing stability for the CT complex within the temperature range of the spectrometer. We can therefore be confident that the two complementary homotrimers are interacting. Conversely, when the two complementary heterotrimers **DAN-NDI-DAN** and **NDI-DAN-NDI** (which both display the CT band as a pure solution) were mixed together in a 1 : 1 ratio, the CT band become less intense than either of the individual components, indicating an interaction between the trimers, but one which decreased the CT interaction. Upon heating up to 45 °C it was found that the CT band decreased linearly by a further 28%, and the solution lost its purple colour (Fig. S10, ESI†). Optical properties reverted upon cooling to room temperature. Thermochromism in aromatic CT complexes[29–31] has been observed to occur *via* structural reorganisation[32] and phase separation.[33] Since phase separation would result in two CT-active compounds, it must be a degree of conformational reorganisation upon interaction of the two compounds which is occurring. It is known that conformational constraints can quench the CT band, despite the formation of nanostructures,[34] and that weaker CT bands are correlated with less well defined relative geometries,[28] and this may the case here, particularly upon heating.

Changes in self-assembly were also observed by microscopy (Fig. 4). The mixture of **$DAN_3$** and **$NDI_3$** produced a patchy film in which clear delineation of levels was seen, with steps of 2.5 nm measured by AFM. This spacing was also seen in MD modelling, with the two molecules joining to give a single plate-like aggregate of a very similar height, with phosphates occupying the surfaces. This is a clear change in self-assembly arising

 

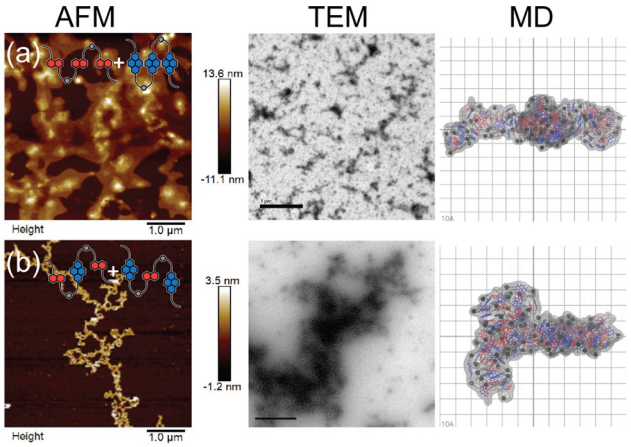


Fig. 4 AFM, TEM and MD modelling of **DAN$_3$/NDI$_3$** (top) and **DAN-NDI-DAN/NDI-DAN-NDI** (bottom) complex nanostructures. Red units in the MD models = **DAN**, blue = **NDI**; dark spheres = phosphates. van der Waals surface shown as a transparent envelope. Further AFM and TEM: Fig S19, S20, S25 and S26 (ESI†).

from the complementary aggregation of these two strands. The heterotrimer mixture was seen to produce a jagged, thread-like network, primarily of height 2–3 nm, although some portions were as high as 6 nm, again in contrast to structures formed by either of the trimers on their own. This is consistent with the MD model which produced a structure consisting of domains with a width of 2–3 nm, but displaying branching regions. Within the MD-modelled clusters, alternating **DAN**/**NDI** stacks were observed on a small scale, but not over longer distances, showing that only local order is present, which might be easily lost upon heating, leading to reduction of the CT band.

We have synthesised sequence-defined **DAN-NDI** phosphodiester trimers using phosphoramidite chemistry. The sequence of aromatic donors and acceptors determines the self-assembly of each strand. When complementary sequences are combined, new self-assembled structures, and thermochromic behaviour, emerge. Although these structures lack long-range order, short-range motifs are sufficient to influence the overall nanostructure. Since phosphoramidite chemistry enables the synthesis of long, information rich strands, this raises possibilities for non-biological sequence-programmed nanotechnology which is orthogonal to biology.

## Conflicts of interest

There are no conflicts to declare.

## Notes and references

1 J.-F. Lutz, M. Ouchi, D. R. Liu and M. Sawamoto, *Science*, 2013, **341**, 1238149.
2 C. A. Hunter and J. K. M. Sanders, *J. Am. Chem. Soc.*, 2002, **112**, 5525–5534.
3 R. S. Lokey and B. L. Iverson, *Nature*, 1995, **375**, 303.
4 R. S. Forgan, J. J. Gassensmith, D. B. Cordes, M. M. Boyle, K. J. Hartlieb, D. C. Friedman, A. M. Z. Slawin and J. F. Stoddart, *J. Am. Chem. Soc.*, 2012, **134**, 17007–17010.
5 H. Y. Au-Yeung, G. D. Pantoş and J. K. M. Sanders, *J. Org. Chem.*, 2011, **76**, 1257–1268.
6 A. Das and S. Ghosh, *Angew. Chem., Int. Ed.*, 2014, **53**, 2038–2054.
7 M. E. Dehkordi, V. Luxami and G. D. Pantoş, *J. Org. Chem.*, 2018, **83**, 11654–11660.
8 G. J. Gabriel, S. Sorey and B. L. Iverson, *J. Am. Chem. Soc.*, 2005, **127**, 2637–2640.
9 K. P. de Carvasal, N. Aissaoui, G. Vergoten, G. Bellot, J.-J. Vasseur, M. Smietana and F. Morvan, *Chem. Commun.*, 2021, **57**, 4130–4133.
10 Z. Zhu, C. J. Cardin, Y. Gan, C. A. Murray, A. J. P. White, D. J. Williams and H. M. Colquhoun, *J. Am. Chem. Soc.*, 2011, **133**, 19442–19447.
11 G. J. Gabriel and B. L. Iverson, *J. Am. Chem. Soc.*, 2002, **124**, 15174–15175.
12 Q. Z. Zhou, M. X. Jia, X. Bin Shao, L. Z. Wu, X. K. Jiang, Z. T. Li and G. J. Chen, *Tetrahedron*, 2005, **61**, 7117–7124.
13 S. De, D. Koley and S. Ramakrishnan, *Macromolecules*, 2010, **43**, 3183–3192.
14 B. Gong, *Acc. Chem. Res.*, 2012, **45**, 2077–2087.
15 M. Morisue, Y. Hoshino, K. Shimizu, M. Shimizu and Y. Kuroda, *Chem. Sci.*, 2015, **6**, 6199–6206.
16 D. Núñez-Villanueva and C. A. Hunter, *Acc. Chem. Res.*, 2021, **54**, 1298–1306.
17 A. A. Sagade, K. V. Rao, U. Mogera, S. J. George, A. Datta and G. U. Kulkarni, *Adv. Mater.*, 2013, **25**, 559–564.
18 M. Probst, S. M. Langenegger and R. Haner, *Chem. Commun.*, 2014, **50**, 159–161.
19 N. Appukutti and C. J. Serpell, *Polym. Chem.*, 2018, **9**, 2210–2226.
20 N. Appukutti, J. R. Jones and C. J. Serpell, *Chem. Commun.*, 2020, **56**, 5307–5310.
21 B. A. Ikkanda, S. A. Samuel and B. L. Iverson, *J. Org. Chem.*, 2014, **79**, 2029–2037.
22 S. M. Langenegger and R. Häner, *ChemBioChem*, 2005, **6**, 2149–2152.
23 M. Vybornyi, Y. Vyborna and R. Häner, *Chem. Soc. Rev.*, 2019, **48**, 4347–4360.
24 B. Baumgartner, A. Svirkova, J. Bintinger, C. Hametner, M. Marchetti-Deschmann and M. M. Unterlass, *Chem. Commun.*, 2017, **53**, 1229–1232.
25 B. A. C. Horta, P. T. Merz, P. F. J. Fuchs, J. Dolenc, S. Riniker and P. H. Hünenberger, *J. Chem. Theory Comput.*, 2016, **12**, 3825–3850.
26 P. C. T. Souza, R. Alessandri, J. Barnoud, S. Thallmair, I. Faustino, F. Grünewald, I. Patmanidis, H. Abdizadeh, B. M. H. Bruininks, T. A. Wassenaar, P. C. Kroon, J. Melcr, V. Nieto, V. Corradi, H. M. Khan, J. Domański, M. Javanainen, H. Martinez-Seara, N. Reuter, R. B. Best, I. Vattulainen, L. Monticelli, X. Periole, D. P. Tieleman, A. H. de Vries and S. J. Marrink, *Nat. Methods*, 2021, **18**, 382–388.
27 T. G. W. Edwardson, K. M. M. Carneiro, C. J. Serpell and H. F. Sleiman, *Angew. Chem., Int. Ed.*, 2014, **53**, 4567–4571.
28 A. J. Zych and B. L. Iverson, *J. Am. Chem. Soc.*, 2000, **122**, 8898–8909.
29 T. Yuan, Y. Xu, C. Zhu, Z. Jiang, H.-J. Sue, L. Fang and M. A. Olson, *Chem. Mater.*, 2017, **29**, 9937–9945.
30 V. C. Wakchaure, L. V. Pillai Goudappagouda, K. C. Ranjeesh, S. Chakrabarty, S. Ravindranathan, P. R. Rajamohanan and S. S. Babu, *Chem. Commun.*, 2019, **55**, 9371–9374.
31 K. Narasimha, *ACS. Appl. Polym. Mater.*, 2020, **2**, 1145–1159.
32 C. D. Wight, Q. Xiao, H. R. Wagner, E. A. Hernandez, V. M. Lynch and B. L. Iverson, *J. Am. Chem. Soc.*, 2020, **142**, 17630–17643.
33 P. M. Alvey, J. J. Reczek, V. Lynch and B. L. Iverson, *J. Org. Chem.*, 2010, **75**, 7682–7690.
34 M. A. Kobaisi, R. S. Bhosale, M. E. El-Khouly, D. D. La, S. D. Padghan, S. V. Bhosale, L. A. Jones, F. Antolasic, S. Fukuzumi and S. V. Bhosale, *Sci. Rep.*, 2017, **7**, 16501.